# The Thermal Entrance Region in Fully Developed Turbulent Flow

**PETER H. ABBRECHT and STUART W. CHURCHILL**

University of Michigan, Ann Arbor, Michigan

**The temperature profile and the local rate of heat transfer from the wall were measured at 0.453, 1.13, 4.12, and 9.97 tube diameters downstream from a step increase in wall temperature for air in fully developed turbulent flow at Reynolds numbers of 15,000 and 65,000 in a 1.52-in. tube. The velocity profile and the pressure were also measured at these lengths.**

**Radial and longitudinal temperature gradients, radial heat fluxes, and eddy diffusivities for heat and momentum transfer were computed from the measurements. The longitudinal temperature gradients at all radii were found to differ significantly from the mixed mean temperature gradient. Although the radial heat flux was a maximum at the wall, the radial heat-flux density, in terms of which the eddy diffusivity for heat transfer is usually defined, was found to go through a maximum near the wall and then to decrease almost linearly across the thermal boundary layer. The eddy diffusivity for heat transfer was found to be independent of length in the thermal entrance region and hence a function only of the fluid motion, as previously hypothesized.**

This paper presents the results of an experimental investigation of heat transfer in the region following a step change in wall temperature in fully developed turbulent flow in a tube. Following such a change in wall temperature, the temperature field in the fluid and the rate of heat transfer from the wall change rapidly, while the velocity field and rate of momentum transfer change only slightly, owing to changes in the physical properties of the fluid with temperature.

The length of tube required for the temperature of the fluid at the center of the tube to change some small arbitrary amount is called the *thermal entrance region*. The thermal entrance region has particular interest because of the high heat transfer coefficients attainable and has received recent attention in connection with heat transfer in nuclear reactors and other compact equipment. The step change in wall temperature in fully developed flow has particular theoretical interest since Tribus and Klein (*20*) have shown that a knowledge of the resulting temperature field permits computation of the rate of heat transfer for any wall-temperature distribution.

Previous experimental investigations of heat transfer in the thermal entrance region have apparently been limited to measurements of the surface temperature, the mixed mean temperature, and the heat flux at the wall. Analytical representations have all assumed that eddy diffusivities measured in fully developed boundary layers are directly applicable in the thermal entrance region.

In this investigation the time-mean temperature and velocity fields were measured as well as the heat flux at the wall in order to provide insight into the mechanism of heat transfer in the entrance region and to test the postulates of previous investigators. The measurements were made in air at Reynolds numbers of approximately 15,000 and 65,000. Temperature differences of less than 30°F. were utilized to minimize changes in the physical properties of the air.

## MATHEMATICAL RELATIONSHIPS

The conservation of momentum in the axial direction in fully developed turbulent flow of a fluid of constant physical properties can be written in terms of the time-mean pressure and velocity with the contribution of the fluctuating components of the velocity expressed as an eddy diffusivity as follows:

$$-\frac{g_o}{\rho}\frac{\partial P}{\partial x}+\frac{1}{r}\frac{\partial}{\partial r}\left[r(\nu+\epsilon_m)\frac{\partial u}{\partial r}\right]=0 \quad (1)$$

Integrating for constant $\partial P/\partial x$ and rearranging yields

$$\frac{\epsilon_m}{\nu}+1=\frac{rg_o}{2\mu}\frac{\partial P}{\partial x}\frac{\partial r}{\partial u}=\frac{r}{a}\frac{dy^+}{du^+} \quad (2)$$

Since the eddy diffusivity is presumed to fall to zero at the wall, Equation (2) can be rewritten as

$$\frac{\epsilon_m}{\nu}+1=\frac{r}{a}\frac{(\partial u/\partial r)_w}{(\partial u/\partial r)} \quad (3)$$

In principle the eddy diffusivity for momentum transfer in fully developed flow can thus be computed for any radius from experimental measurements of the radial velocity profile only. However the longitudinal pressure gradient can be measured more accurately than the radial velocity gradient at the wall, and Equation (2) is therefore more practical for computations than Equation (3).

The conservation of energy can similarly be written in terms of time-mean temperature and velocities, and axial and radial eddy diffusivities for heat transfer as follows:

$$u\frac{\partial t}{\partial x}=\frac{\partial}{\partial x}\left[(K+\epsilon_h')\frac{\partial t}{\partial x}\right]+\frac{1}{r}\frac{\partial}{\partial r}\left[r(K+\epsilon_h)\frac{\partial t}{\partial r}\right] \quad (4)$$

The first term on the right side of Equation (4) has been shown to be negligible under most circumstances (*16*) and will be dropped for simplicity. Integration then yields

$$\frac{\epsilon_h}{K}+1=\frac{1}{rK}\frac{\partial r}{\partial t}\int_o^r u\frac{\partial t}{\partial x}rdr \quad (5)$$

The radial eddy diffusivity for heat transfer can also be expressed in terms of the local radial heat-flux density:

$$\frac{\epsilon_h}{K}+1=\frac{q}{k}\frac{\partial r}{\partial t} \quad (6)$$

The radial heat-flux density is discussed in detail by Churchill and Balzhiser (*5*). Comparison of Equations (5) and (6) indicates that subject to the assumptions inherent in Equation (5)

$$q=\frac{\rho c}{r}\int_o^r u\frac{\partial t}{\partial x}rdr \quad (7)$$

For a constant heat flux at the wall and a fully developed temperature distribution $\partial t/\partial x$ is constant with respect to radius and length (*16*). For the thermal entrance region and for other boundary conditions $\partial t/\partial x$ varies with radius. Determination of the eddy diffusivity for heat transfer for such conditions thus requires measurement of the longitudinal temperature profile as well as the radial temperature and velocity profiles.

The local heat transfer rate at the wall is expressed in the customary form in terms of $hD/k$ where

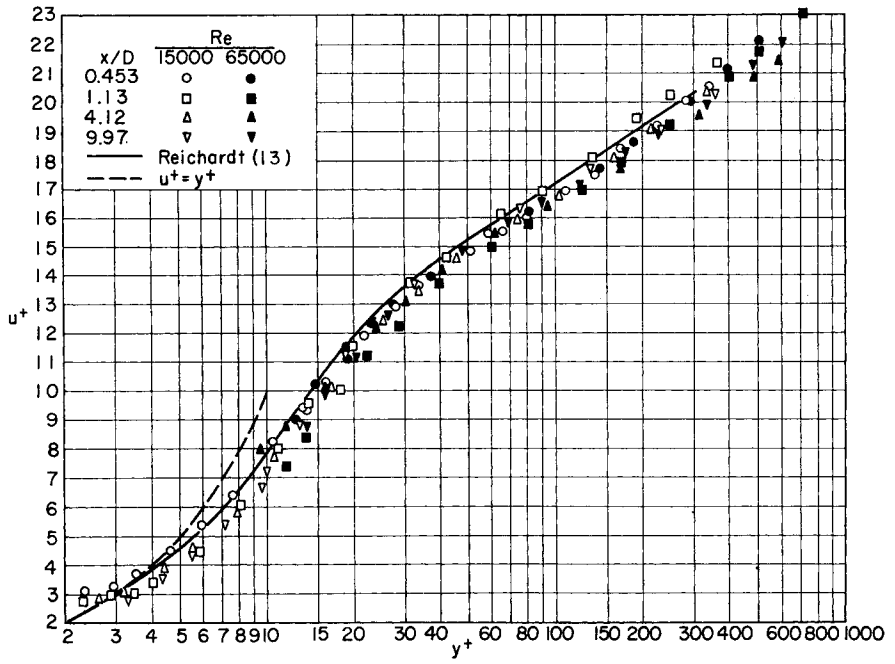


Fig. 1. Velocity-distribution data.

$$h = q_w/(T_w - T_b) \qquad (8)$$

and

$$T_b = \int_0^1 T \left(\frac{u}{u_b}\right) d\left(\frac{r}{a}\right)^2 \qquad (9)$$

## EXPERIMENTAL APPARATUS

Air from a 90 lb./sq. in. gauge supply main passed through a filter; a flow-control valve; a calming section; a converging nozzle; a 66 in.–long unheated tube; a heated tube of variable length; a 1 in.–long, 0.19 in.–thick, heated copper tube serving as a calorimeter; another unheated tube containing an orifice; and finally into the atmosphere. The entrance and test sections of tube were honed to an inside diameter of 1.520 in. with a 30-$\mu$ in. finish.

The nozzle and unheated tube yielded essentially fully developed turbulent flow. Four interchangeable heating tubes were utilized so that total heating distance to the center of the calorimeter was 0.453, 1.13, 4.12, or 9.97 tube diameters. A steam jacket was used to heat the two longer tubes and electrical resistance coils to heat the two shorter tubes and the calorimeter. A 0.2 in. thick plastic disk insulated the entrance section from the heating section. The calorimeter was insulated from the adjacent sections of tube with 0.015 in. thick plastic disks and was surrounded by a guard heater. The sections of tube were aligned by means of carefully machined male and female joints.

A traversing mechanism was located downstream from the calorimeter with a probe extending upstream to the midplane of the calorimeter. The tip of the probe consisted of a 140-mil–long 3-mil wire, the center 40 mils of which were etched to 0.3 mil. This probe was used as a hot-wire anemometer to measure the velocity profile and as a resistance thermometer to measure the temperature profile. The heat flux through the calorimeter wall to the air stream was determined from voltage and current readings on the calorimeter heating coil.

The inlet air temperature was measured with a thermocouple in the calming section and the orifice temperature with a thermometer. Thermocouples were located at a number of azimuthal and longitudinal points in the wall of the heating section and calorimeter. Pressure-drop measurements were made with a micromanometer between taps located at 1, 3, 5, 15, 30, 44.5, 61, and 65 in. from the nozzle and at the outlet of the calorimeter.

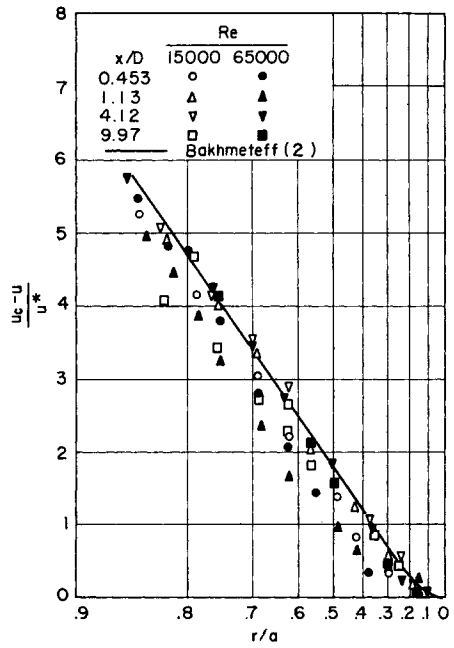


Fig. 2. Velocity deficiency.

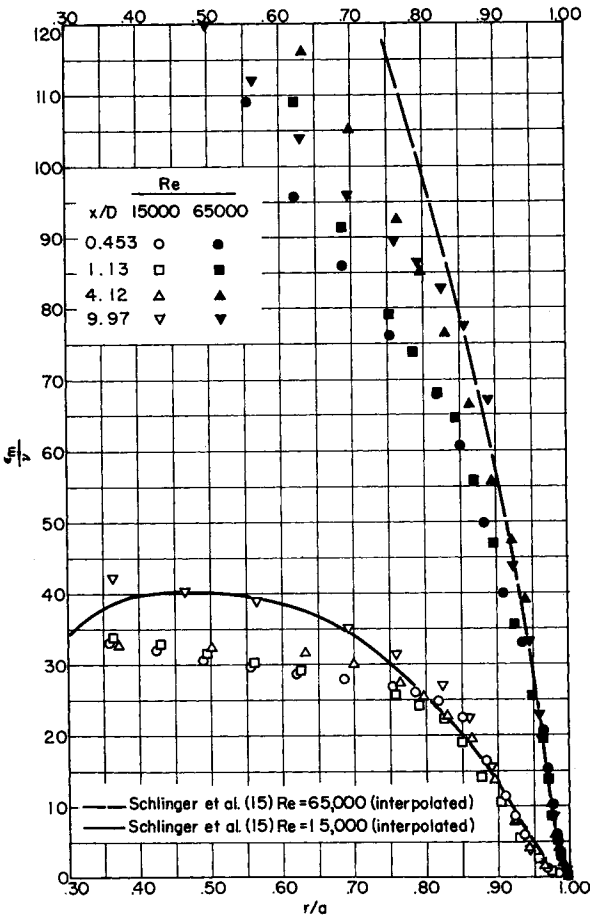


Fig. 3. Eddy diffusivity for momentum transfer.

Calibration of the measuring devices and further equipment details are given in reference 1. The raw data are preserved insofar as possible in the subsequent correlations to avoid prejudicing the results.

## EXPERIMENTAL DATA

The heat flux at the wall and the radial temperature and velocity profiles were measured at the four stations at Reynolds numbers of approximately 15,000 and 65,000. No significant difference was observed in velocities measured during heating and nonheating runs, and the reported velocity data were obtained during the heating runs. The pressure gradient was determined for each run by averaging the differential measurements obtained at a number of positions along the tube. The experimental conditions and over-all data for the eight runs are summarized in Table 1.* The physical properties of air were taken from reference 9 except for density, which was computed from the ideal gas law.

The uncertainty in the measured velocities varied from about 0.5% at the center line up to perhaps 5% at a velocity of 7 ft./sec. The uncertainty in the measured temperatures is estimated at ±0.2°F. The location of the probe was known within about ±0.0005 in. The pressure gradient was reproducible to within less than 1% at a Reynolds number of 65,000 and less than 3% at 15,000. The heat flux obtained from the calorimeter is believed to be dependable within 3% at an $x/D$ of 10 but to be somewhat less certain at lower values of $x/D$.

## MOMENTUM TRANSFER

The measured pressure gradients agreed within 2% with the correlation of Moody (*10*) for fully developed flow in smooth pipe. Velocity data for all eight runs are plotted in Figure 1 as $u^+$ vs. $y^+$. Some overlying experimental points were omitted for clarity. The data for $y^+ > 3$ are in good agreement with those of previous investigations as indicated by the curve representing the measurements of Reichardt and others (*13*) and appear to extrapolate satisfactorily to zero velocity at the wall. The high velocities for $y^+ < 3$ are apparently due to heat transfer from the heated wire to the wall. Although empirical corrections have been proposed for this effect, their accuracy is questionable and such corrections would add little to the information obtained from this investigation.

The velocities in Figure 1 show a slight variation with $x/D$, indicating that the boundary layer was still developing even for these entrance lengths of 44 diam. and greater. As noted by Rothfus and Monrad (*14*) and others, a slight dependence on Reynolds number is also apparent. The incomplete development of the boundary layer can be examined more critically in Figure 2 in which the dimensionless velocity deficiency $(u_c - u)/u^*$ is plotted. Some development is indicated, but the data agree quite well with the curve given by Bakhmeteff (*2*) for fully developed flow.

The velocity data were differentiated graphically, and the velocity gradients obtained from equal area curves were used to compute the eddy diffusivity for momentum transfer in Figure 3. Curves obtained by interpolating the results of Schlinger *et al.* (*15*) for flow in circular pipes are included in Figure 3 for comparison. The agreement between these curves and the data of this investigation is good. Figure 3 is a still more critical test of the development of the boundary layer. The scatter of the data below the curves for $r/a$ less than 0.8 is to be expected because of the very small velocity gradient and is not believed to be significant.

Equation (2) suggests that a plot of $[(\epsilon_m/\nu) + 1]\ (a/r)$ vs. $y^+$ would not show dependence on the Reynolds number if $u^+$ were a function of $y^+$ only. The data in Figure 3 are replotted in this form in Figure 4. Despite the magnification of the actual dependence of $u^+$ on the Reynolds number for a given $y^+$ by the differentiation which leads from Figure 1 to Figure 4, a reasonably compact correlation is obtained.

## HEAT TRANSFER

The heat fluxes obtained from the calorimeter were corrected for heat losses to the surroundings and through the plastic disks isolating the test sec-

*Tabular material has been deposited as document 6260 with the American Documentation Institute, Photoduplication Service, Library of Congress, Washington 25, D. C., and may be obtained for $2.50 for photoprints or $1.75 for 35-mm. microfilm.

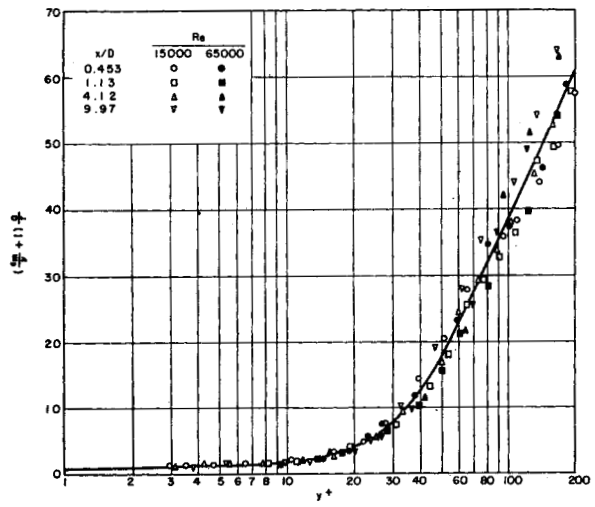


Fig. 4. Generalized correlation of eddy diffusivity for momentum transfer.

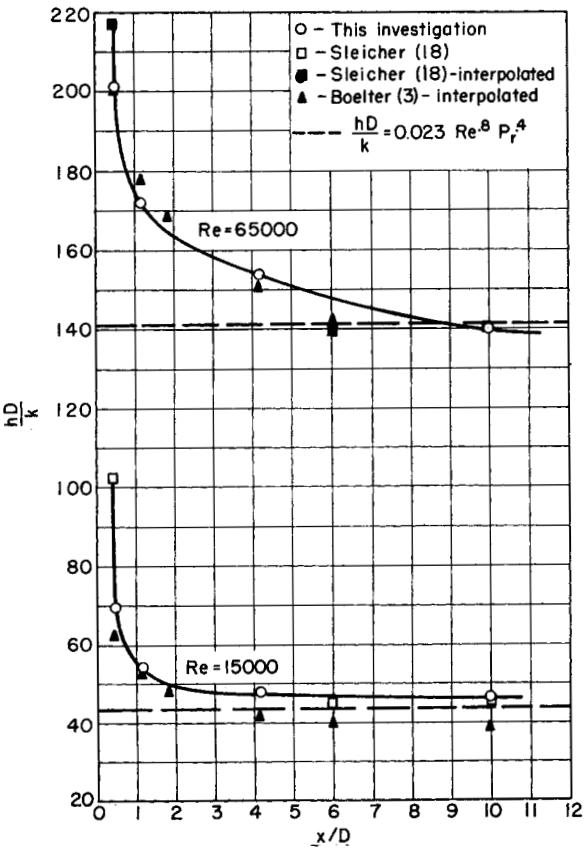


Fig. 5. Local Nusselt number.

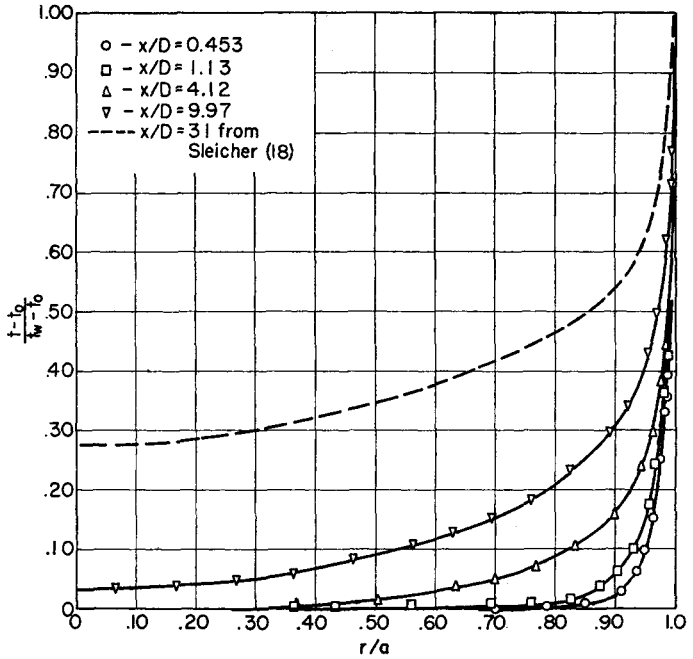


Fig. 6. Temperature distribution data for $N_{Re} = 15{,}000$.

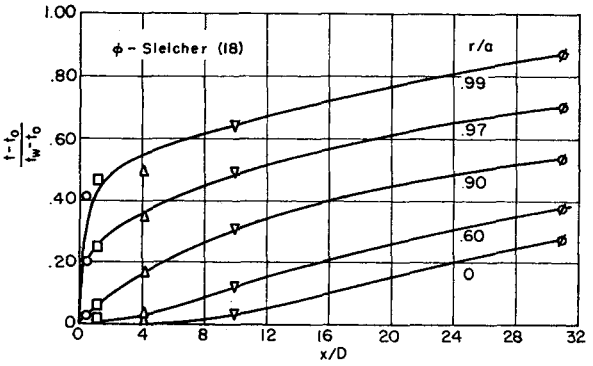


Fig. 7. Longitudinal temperature profiles for $N_{Re} = 15{,}000$.

tion. The computed loss through the plastic disks was in every case less than 3%. The heat losses to the surroundings were estimated from heat flux measurements with no flow. This correction was 12.5% or less at a Reynolds number of 15,000 and 4.3% or less at a Reynolds number of 65,000.

Since the corrected heat fluxes were for 1-in. segments of the tube, it was necessary to obtain the point fluxes from an equal-area curve through a plot of the segmental rate vs. length. The bulk temperature at each station was obtained by graphical integration of the temperature and velocity data according to Equation (9). The local heat transfer coefficient defined by Equation (8) and $hD/k$ were then calculated. These quantities are all included in Table 1.

Figure 5 plots the local Nusselt number as a function of heated length. Excellent agreement with the data of Sleicher (*18*) and Boelter, Young, and Iverson (3) can be noted. The asymptotic values predicted by the empirical equation of Dittus and Boelter (*8*) for long tubes are also shown. The Nusselt number appears to have attained close to its asymptotic value at an $x/D$ of 10.

The temperature-distribution data is illustrated for $N_{Re}$ of 15,000 in Figure 6. A curve representing the data of Sleicher (*18*) at an $x/D$ of 31 is included. The radial temperature gradients were obtained by graphical differentiation of the data. The longitudinal temperature profiles shown in Figure 7 were obtained by cross plotting the temperature-distribution data. The longitudinal temperature gradients shown in Figure 8 were obtained by differentiating the longitudinal temperature profiles. The mixed mean temperature gradient was obtained from the smoothed heat flux; that is

$$\frac{\partial[(t_b-t_o)/(t_w-t_o)]}{\partial(x/a)} = \frac{2q_w}{\rho c u_b (t_w-t_o)} \quad (10)$$

It is apparent from Figure 8 that the longitudinal gradients at all radii differ from the mixed mean gradient even for an $x/D$ of 10. Similar results were obtained at a Reynolds number of 65,000. However because of the absence of data for $x/D$ greater than 9.97 the longitudinal gradients at $x/D$ of 9.97 were defined with less certainty than at a Reynolds number of 15,000.

The radial heat flux density was computed from the following modified forms of Equation (7):

$$\frac{q}{q_w}\frac{r}{a} = 1 - \int_{r/a}^{1} \frac{u}{u_b}\frac{(\partial t/\partial x)}{(\partial t_b/\partial x)} d\left(\frac{r}{a}\right)^2 = \int_{o}^{r/a} \frac{u}{u_b}\frac{(\partial t/\partial x)}{(\partial t_b/\partial x)} d\left(\frac{r}{a}\right)^2 \quad (11)$$

for the regions near the wall and center respectively. The results are illustrated for a Reynolds number of 15,000 in Figure 9. The data points are omitted since the integration which yields Figure 9 is inherently a smoothing process. Although the radial heat flux decreases monotonically from the wall, the radial flux density, in terms of which the eddy diffusivity for heat transfer can be defined [Equation (6)], is observed to go through a maximum and then to decrease almost linearly across the thermal boundary layer. This behavior is due to the opposing effects of longitudinal transfer and decreasing circumference.

The eddy diffusivity for heat transfer was next computed from a modified form of Equation (6),

$$\frac{\epsilon_h}{K} + 1 = \frac{q_w}{K}\cdot\frac{\partial r}{\partial t}\cdot\frac{q}{q_w} \quad (12)$$

by means of the heat flux density at the wall derived from the calorimeter measurements. The computed points are plotted vs. $r/a$ in Figure 10. The data for $x/D$ of 9.97 at a Reynolds number of 65,000 are omitted because of the previously noted uncertainty in the longitudinal temperature gradients. When the effect of the slightly changing velocity profile is considered, it is apparent that the eddy diffusivity for heat transfer is not a significant function of length in the thermal entrance region. Curves representing the data of Sleicher (*18*) for a fully developed thermal boundary layer in a tube and the data of Page *et al.* (*11*) for fully

Table 1. Experimental Conditions and Results

| Run No. | x/D | w, lb/hr | $t_o$, °F | $t_w$, °F | $t_b$, °F | $4w/\pi D\mu_b$ | $q_w$, Btu/(hr)(sq ft) | h, Btu/(hr)(sq ft)°F | $hD/k_b$ |
|---|---|---|---|---|---|---|---|---|---|
| 1 | 0.453 | 66.6 | 79.35 | 104.01 | 79.60 | 15000 | 207 | 8.45 | 69.4 |
| 2 | 1.13 | 66.0 | 82.17 | 109.70 | 83.02 | 14780 | 174 | 6.53 | 53.7 |
| 3 | 4.12 | 66.4 | 83.78 | 110.80 | 85.85 | 14860 | 147 | 5.87 | 47.8 |
| 4 | 9.97 | 65.8 | 83.49 | 108.48 | 87.35 | 14700 | 121 | 5.72 | 46.6 |
| 5 | 0.453 | 285.0 | 81.48 | 104.46 | 81.85 | 64100 | 551 | 24.4 | 201 |
| 6 | 1.13 | 287.0 | 84.24 | 113.65 | 84.74 | 64200 | 601 | 20.8 | 172 |
| 7 | 4.12 | 284.0 | 80.40 | 106.69 | 82.05 | 63800 | 462 | 18.7 | 154 |
| 8 | 9.97 | 290.0 | 81.81 | 107.49 | 84.55 | 64900 | 390 | 17.0 | 140 |

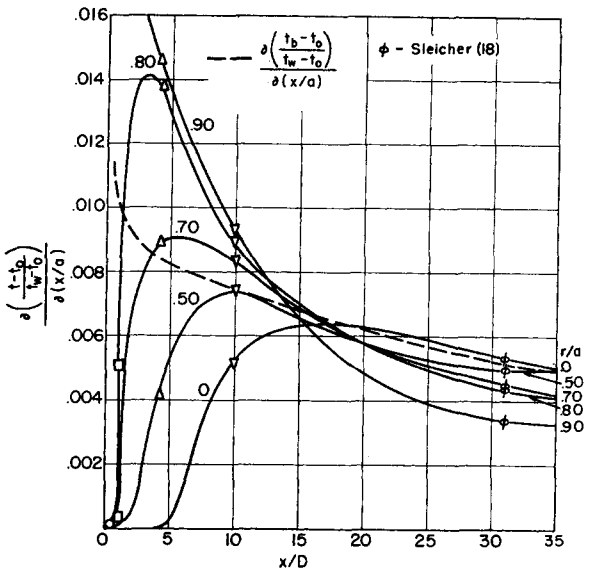


Fig. 8. Longitudinal temperature gradients for $N_{Re}$ = 15,000.

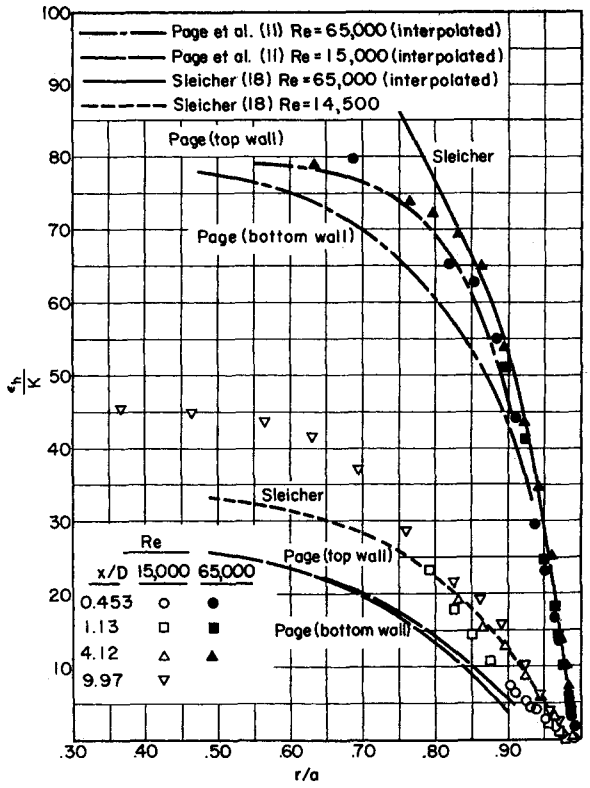


Fig. 10. Eddy diffusivity for heat transfer.

developed heat transfer between parallel plates are included in Figure 10 for comparison. The curve of Sleicher for a Reynolds number of 14,500 is reproduced directly. The curves for a Reynolds number of 65,000 were obtained by cross plotting, interpolating, and converting the reported results of Sleicher and Page *et al.* The agreement with these previous experiments is excellent for $r/a$ greater than 0.8 and is reasonable for smaller $r/a$, considering the smaller and hence more uncertain temperature gradients.

The data are replotted as $[(\epsilon_h/K)+1]\ (a/r)$ vs. $y^+$ in Figure 11. Again, as for momentum transfer, a reasonably general correlation for all Reynolds numbers is obtained in this form. The curve in Figure 11 coincides with the smoothed results of Cavers (*4*) for heat transfer between parallel plates which extend to $y^+$ of 46.

Figure 12 plots the ratio of the eddy diffusivities for heat and momentum transfer as a function of position. Curves representing the results of Sleicher (*18*) and Page *et al.* (*12*) are included. This plot is a very critical test of the data since the ordinate involves the ratio of the derivatives of two independently measured quantities. Accordingly the scatter is not believed to be unreasonable; it appears to be random with respect to Reynolds number as well as to length, although Sleicher and Page *et al.* infer small effects for the Reynolds number from their data. The ratio $\epsilon_h/\epsilon_m$ has a value of 1.0 to 1.5 in the turbulent core but increases rapidly near the wall.

## DISCUSSION

The agreement of the velocity data for all four test stations with the correlations of previous investigators in Figure 1 indicates that essentially fully developed turbulent motion was established. The independence of the motion near the wall from $x/D$ is further indicated in Figures 2, 3, and 4. The comparison in Figure 5 of the local heat transfer rate data with that of previous investigators for a step function in wall temperature in fully developed flow is evidence that the thermal boundary conditions as well as the flow conditions were representative.

The temperature-distribution data are difficult to interpret directly. However the deviation of the longitudinal temperature gradients at all radii from the mixed mean temperature gradient, even for an $x/D$ of 10 where $hD/k$ has approached its asymptotic value, is significant since theoretical models frequently have postulated the form of these gradients. The radial variation of the heat flux density illustrated in Figure 9 is also of particular interest since temperature-distribution data and analytical results have apparently not been expressed in this form and since the radial heat flux density has been assumed to be constant in the theoretical developments of Deissler (*6, 7*) and others.

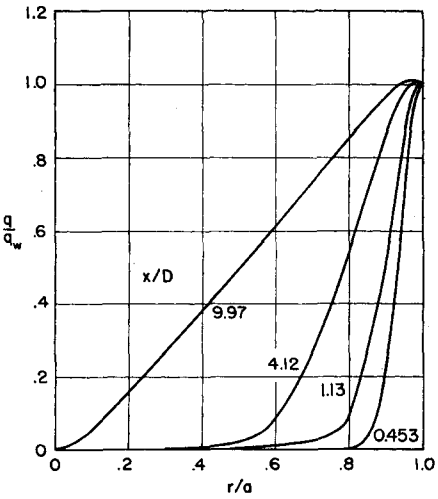


Fig. 9. Radial heat-flux density for $N_{Re}$ = 15,000.

The eddy diffusivity for heat transfer in fully developed turbulent flow is shown in Figures 10, 11, and 12 to be invariant with length in the thermal entrance region following a step function in temperature and hence to be a function of the fluid motion only. The reasonable agreement noted in Figures 10, 11, and 12 with the results for heat transfer between parallel plates is further evidence of the independence of the eddy diffusivity from the temperature field. These observations confirm the hypothesis made by Deissler (*7*), Sleicher and Tribus (*19*), Seban and Shimazaki (*17*), Tribus and Klein (*20*), and others in theoretical derivations for the thermal entrance region.

The dimensionless groups $[(\epsilon_m/\nu)+1]\ a/r$ and $[(\epsilon_h/K)+1]\ a/r$ are observed in Figures 4 and 11 to be single valued functions of $y^+$ for both Reynolds numbers within the certainty of the data. However the rapid increase indicated in Figure 12 for the ratio of the eddy diffusivities for heat and

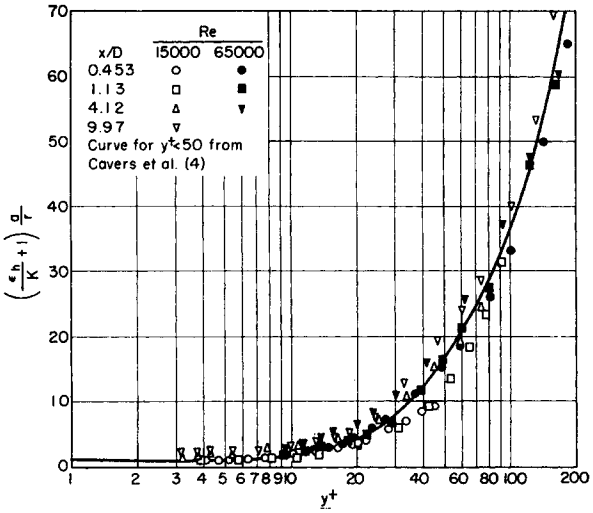


Fig. 11. Generalized correlation for eddy diffusivity for heat transfer.

momentum transfer near the wall challenges the validity and generality of theoretical models which postulate a constant ratio.

## NOTATION

$a$ = radius of tube, ft.
$c$ = heat capacity, B.t.u./(lb.)(°F.)
$D$ = diameter of tube, ft.
$g_c$ = conversion factor = 32.17 (lb.)(ft.)/(lb.-force)(sec.)$^2$
$h$ = heat transfer coefficient, B.t.u./(sec.)(sq.ft.)(°F.)
$k$ = thermal conductivity, B.t.u./(sec.)(sq.ft.)(°F./ft.)
$K$ = $k/\rho c$ = thermal diffusivity, sq. ft./sec.
$N_{Pr}$ = $c\mu/k$ = Prandtl number
$N_{Re}$ = $4w/\pi D\mu$ = Reynolds number
$P$ = pressure, lb.-force/sq. ft.
$q$ = heat flux density, B.t.u./(sec.)(sq.ft.)
$r$ = radial distance from axis of tube, ft.
$t$ = temperature, °F.
$u$ = velocity, ft./sec.
$u^*$ = $\sqrt{\frac{Dg_c}{4\rho}\left(-\frac{\partial P}{\partial x}\right)}$ = friction velocity, ft./sec.
$u^+$ = $u/u^*$ = dimensionless velocity
$x$ = heated length, ft.
$y$ = distance from wall, ft.
$y^+$ = $yu^*/\nu$ = dimensionless distance from wall
$w$ = flow rate = lb./sec.

### Greek Letters

$\epsilon_h$ = radial eddy diffusivity for heat transfer, sq. ft./sec.
$\epsilon'_h$ = longitudinal eddy diffusivity for heat transfer, sq. ft./sec.
$\epsilon_m$ = eddy diffusivity for momentum transfer, sq. ft./sec.
$\theta$ = $(t-t_o)/(t_w-t_o)$ = dimensionless temperature
$\mu$ = viscosity, lb./(ft.)(sec.)
$\nu$ = $\mu/\rho$ = kinematic viscosity, sq. ft./sec.
$\rho$ = density, lb./cu. ft.

### Subscripts

$b$ = mixed mean
$c$ = center
$o$ = initial
$w$ = wall

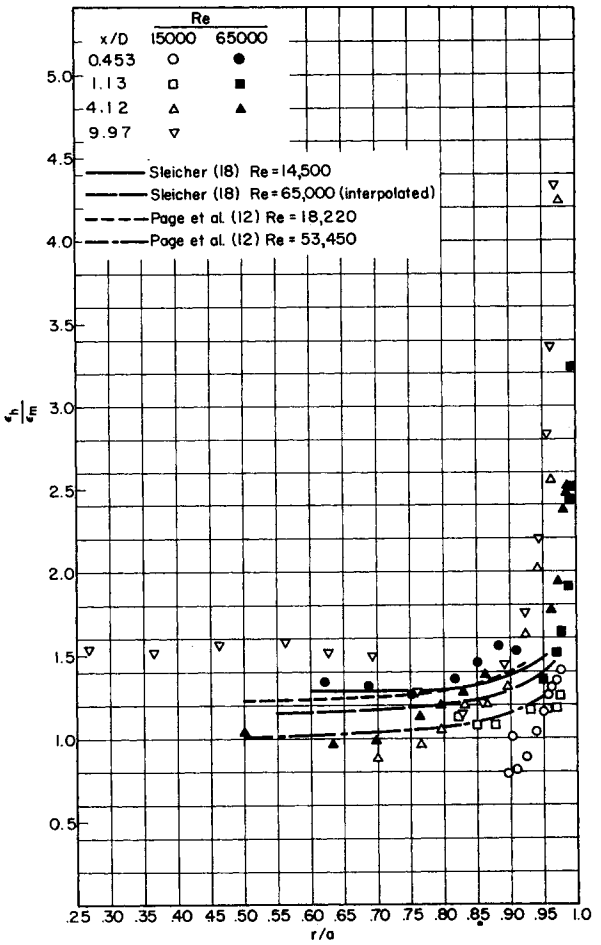


Fig. 12. Ratio of eddy diffusivities for heat and momentum transfer.

## LITERATURE CITED


1. Abbrecht, P. H., Ph.D. thesis, Univ. Mich., Ann Arbor (1956).
2. Bakhmeteff, B., "Mechanics of Turbulent Flow," Princeton Univ. Press, Princeton, New Jersey (1941).
3. Boelter, L. M. K., G. Young, and H. W. Iverson, *Natl. Advisory Comm. Aeronaut. Tech. Note 1451*, Washington, D. C. (1948).
4. Cavers, S. D., N. T. Hsu, W. G. Schlinger, and B. H. Sage, *Ind. Eng. Chem.*, **45**, 2139 (1953).
5. Churchill, S. W., and R. E. Balzhiser, *Chem. Eng. Progr. Symposium Ser. No. 29*, **55**, 127 (1959).
6. Deissler, R. G., *Natl. Advisory Comm. Aeronaut. Rept. 1210*, Washington, D. C. (1955).
7. ———, *Trans. Am. Soc. Mech. Engrs.*, **77**, 1221 (1955).
8. Dittus, F. W., and L. M. K. Boelter, *Univ. Calif. Pubs. Engr.*, **2**, 443 (1930).
9. John Hopkins Univ., Applied Phys. Lab., Silver Spring, Md., "Handbook of Supersonic Aerodynamics," Navord Rept. 1488, Vol. 5, Washington Bureau of Ordnance (1953).
10. Moody, L. F., *Trans. Am. Soc. Mech. Engrs.*, **66**, 671 (1944).
11. Page, F., Jr., W. H. Corcoran, W. G. Schlinger, and B. H. Sage, *Ind. Eng. Chem.*, **44**, 419 (1952).
12. Page, F., Jr., W. G. Schlinger, D. K. Breaux, and B. H. Sage, *ibid.*, 424 (1952).
13. Reichardt, H., *Natl. Advisory Comm. Aeronaut. Tech. Memo. 1047*, Washington, D. C. (1943).
14. Rothfus, R. R., and C. C. Monrad, *Ind. Eng. Chem.*, **47**, 1147 (1955).
15. Schlinger, W. G., V. J. Berry, J. L. Mason, and B. H. Sage, *ibid.*, **45**, 662 (1953).
16. Schneider, P. J., *Trans. Am. Soc. Mech. Engrs.*, **79**, 765 (1957).
17. Seban, R. A., and T. T. Shimazaki, *ibid.*, **73**, 803 (1951).
18. Sleicher, C. A., Jr., Ph.D. thesis, Univ. Mich., Ann Arbor (1955); *Trans. Am. Soc. Mech. Engrs.*, **80**, 693 (1958).
19. ———, and Myron Tribus, *Trans. Am. Soc. Mech. Engrs.*, **79**, 789 (1957).
20. Tribus, Myron, and J. S. Klein, "Heat Transfer," pp. 211-235, Univ. Press, Ann Arbor, Michigan (1953).


*Manuscript received July 29, 1957; revision received September 30, 1959; paper accepted October 5, 1959. Paper presented at A.I.Ch.E. Baltimore meeting.*